J. Shanghai Jiao Tong Univ. (Sci.), 2023, 28(2): 172-179
https://doi.org/10.1007/s12204-022-2462-1

Synthesis and Characterization of Copper Doped Zinc Oxide Thin Films Deposited by RF/DC Sputtering Technique

KHAN Mohibul, *ALAM Md. Shabaz*, *AHMED Sk. Faruque**
(Nanoscience Laboratory, Department of Physics, Aliah University, Kolkata 700160, India)

Abstract: Undoped and copper (Cu) doped zinc oxide ($Zn_{1-x}Cu_xO$, where $x = 0$—0.065) nano crystal thin films have been deposited on glass substrate via RF/DC reactive co-sputtering technique. The aim of this work is to investigate the crystal structure of ZnO and Cu doped ZnO thin films and also study the effect of Cu doping on optical band gap of ZnO thin films. The identification and confirmation of the crystallinity, film thickness and surface morphology of the nano range thin films are confirmed by using X-ray diffractometer (XRD), scanning electron microscope and atomic force microscope. The XRD peak at a diffractive angle of 34.44° and Miller indices at (002) confirms the ZnO thin films. Crystallite size of undoped ZnO thin films is 27 nm and decreases from 27 nm to 22 nm with increasing the atomic fraction of Cu (x_{Cu}) in the ZnO thin films from 0 to 6.5% respectively, which is calculated from XRD (002) peaks. The different bonding information of all deposited films was investigated by Fourier transform infrared spectrometer in the range of wave number between 400 cm^{-1} to 4 000 cm^{-1}. Optical band gap energy of all deposited thin films was analyzed by ultraviolet visible spectrophotometer, which varies from 3.35 eV to 3.19 eV with the increase of x_{Cu} from 0 to 6.5% respectively. Urbach energy of the deposited thin films increases from 115 meV to 228 meV with the increase of x_{Cu} from 0 to 6.5% respectively.
Key words: Cu-ZnO thin films, RF/DC sputtering technique, X-ray diffraction, atomic force microscope, optical property, Urbach energy
CLC number: O 484 **Document code:** A

0 Introduction

In the last few decades, semiconductor materials are very important for extensive range of applications in the field of science and technology for commercial and non-commercial purposes due to their variable band gap and short-range wavelength. II-VI chalcogenide semiconductors are composed of metals and chalcogens, which belong to group II and group VI elements respectively. ZnO is an environmentally safe n-type II-VI chalcogenide semiconductor economic material whose direct large band gap is 3.37 eV and high exciton binding energy is 60 meV at room temperature of 30 °C[1-3]. ZnO thin films possess properties of piezoelectric oscillators due to their hexagonal wurtzite crystallite structure[1,4-5]. This type of metal chalcogenide II-VI semiconductor thin films has been broadly discussed due to their wide applications in optoelectronic devices such as solar cells, photo detectors and thin-film transistor[1-3,6-8]. ZnO exhibits some additional aspects and many natural advantages such as non-toxic, good transparency, prominent electron mobility, chemical stability and well luminescence property at room temperature[1-2]. Due to these tremendous properties, ZnO thin films are used as ultraviolet protectors, gas sensing devices, antibacterial coatings, cancer treatment, photo catalysis, light emitting diodes, spintronics, high mobility transistor, transparent conducting oxides, schottky diodes, drug delivery devices, flat panel displays, surface acoustic devices, computer screen, high electron mobility, smart phone display, photo voltaic cells, smart windows, laser diodes, varistors, chemical sensors and transparent electrodes[1-4,8-14]. Different types of dopants such as Fe, Sb, Al, Mn, Co, Ni, In, Ga, Sn, Ag, Au, N, Mo, Ti, V and Cu doped with ZnO use physical and chemical techniques for enhancement of some basic properties such as physical, electrical, chemical, dielectric, magnetic and optical[1-3,8,13,15-17]. Cu is an interesting remarkable metal among all dopants for its low cost, non-toxic and naturalistic behavior. Cu also possesses a rare form of the smallest mismatch size between Cu and Zn, which leads to minimum formation energy. Cu and Zn both have same electronic shell configuration because of their nearly same physical and chemical properties.

Received: 2021-05-21 **Accepted:** 2021-07-05
Foundation item: the Maulana Azad National Fellowship (MANF) Scheme of University Grants Commission, New Delhi, India
***E-mail:** fahmed.phys@aliah.ac.in

Electrons can be freely moved from Cu layer to ZnO layer as there is no obstacle between Cu and ZnO layer to run the electrons[3,13]. In the industrial application purposes, Cu doped ZnO films have played an important role in finding out the leakage of hazardous gases like liquefied petroleum gas[10,18].

In recent years, many researchers have used physical and chemical techniques to synthesize pure and Cu doped ZnO thin films such as dip coating, chemical bath deposition, low temperature aqueous solution route, chemical vapour deposition, electron beam evaporation, chemical co-precipitation method, sol-gel preparation, successive ionic layer absorption and reaction (SILAR), spray pyrolysis, hydrothermal method, screen printing, molecular beam epitaxy, thermal evaporation, radio frequency (RF) sputtering, direct current (DC) sputtering, metal organic chemical vapor deposition, pulsed laser deposition, photo chemical deposition, simultaneous DC and RF magnetron sputtering techniques, electrochemical deposition, and co-reactive magnetron sputtering techniques[1-2,13,15,19-21].

RF and DC co-reactive magnetron sputtering technique is a highly advisable method for the formation of nano range thin films. This process has various advantages such as best quality of thin films over conventional methods, large surface area coverage, low-temperature growth, and direct control of film thickness and surface morphology. In the current work, we report the outcome of ZnO and Cu doped ZnO thin films by reactive co-sputtering technique where ZnO target is used in RF shutter and Cu metal target is used in DC shutter simultaneously. The ZnO thin films have been doped with different atomic fraction (x_{Cu}) for the better improvement of the structural and optical properties of the newly formed nano crystal thin films.

All deposited thin films were characterized and analyzed by using X-ray diffractometer (XRD), energy-dispersive X-ray analyzer (EDAX), Fourier transform infrared (FT-IR) spectrometer, atomic force microscope (AFM), and ultraviolet visible (UV-Vis) spectrophotometer. Optical transparency as well as the optical band gap energy was calculated from the transmittance spectra of the deposited films by using UV-Vis spectrophotometer. The change in optical transmittance, band gap energy and Urbach energy with x_{Cu} in the ZnO thin films has been explored in detail.

1 Experimental Details

1.1 Materials and Deposition Techniques

Cu doped ZnO thin films have been synthesized on commercial glass substrate by using reactive co-sputtering deposition technique with the variation of x_{Cu} from 0 to 6.5% respectively at room temperature of 30 °C. All films are deposited for 30 min. ZnO target [purity of 99.999%, diameter of 53.975 mm (2.125 inch), and thickness of 2 mm] and Cu target [purity of 99.999%, diameter of 53.975 mm (2.125 inch), and thickness of 2 mm] were purchased from Sigma-Aldrich Company for source materials. Commercial glass substrate with a size of 75 mm × 25 mm × 1.45 mm was used for synthesis of pure ZnO and Cu doped ZnO thin films by using co-reactive magnetron sputtering technique. Before starting the deposition, all glass substrates were ultrasonically cleaned in acetone for 15 min at 40 °C and rinsed thoroughly with double distilled water 2—3 times continuously and then dried with hot air gun.

ZnO target and Cu metal target were sputtered by RF power and DC power respectively. Before starting the thin-film deposition, the impurities of both targets were washed and removed by pre-sputtering using argon gas (Ar) for 15 min. First, the deposition chamber was evacuated by rotary pump and then turbo pump. The base pressure of the deposition chamber was maintained at 4×10^{-4} Pa using turbo pump. The mass flow controller (MFC) key was used for entering and maintaining the Ar and O_2 into the evacuated chamber at 12 cm^3/min and 4 cm^3/min respectively, which were fixed with the variation of x_{Cu}. As Ar is a good sputtering gas, for this purpose argon is used here. O_2 is used for maintaining the oxygen rich growth environment, which is important for reducing the intrinsic donor defects. Also both gases were used for maintaining the working pressure at 2.5 Pa. Substrates were moving at 2 r/min for good arrangement of atom and molecules, good surface morphology, and uniform film thickness. Distance between cathode shutter and substrate holder was fixed at 7 cm for better thin-film deposition. The deposition was started by RF power set up at 80 W, and DC voltage varying from 200 V to 260 V. The x_{Cu} varies from 2.3% to 6.5% with the variation of DC voltages from 200 V to 260 V. Only RF power was supplied in ZnO target for the deposition of undoped ZnO thin films. Details of deposition conditions are given in Table 1.

Table 1 Synthesis conditions maintained for the formation of nano crystal thin films

Deposition parameter	Value
Base pressure/Pa	4×10^{-4}
Working pressure/Pa	2.5
Ar flow/($\mathrm{cm}^3 \cdot \mathrm{min}^{-1}$)	12
O_2 flow/($\mathrm{cm}^3 \cdot \mathrm{min}^{-1}$)	4
Deposition temperature/°C	30
Substrate rotation speed ($\mathrm{r} \cdot \mathrm{min}^{-1}$)	2
RF power/W	80
DC voltage/V	200, 230, 260
Deposition time/min	30
Distance between target and substrate holder/mm	70

1.2 Characterizations

The compositional, structural, morphological and optical characteristics of undoped ZnO and Cu doped ZnO nano thin films were analyzed. The chemical composition of undoped ZnO and Cu doped ZnO thin films was investigated by EDAX (Oxford, model-7582). The structural crystallinity of all films was analyzed by using XRD (Bruker, D-8 Advance). The surface morphological characteristics of all nano crystal thin films were investigated by using ambient based multimode AFM (Bruker, MultiMode-8). All AFM measurements were done in contact mode. A silicon probe having a radius of curvature of 10 nm, and height of 15 μm with a standard chip size of 1.6 mm × 1.6 mm × 0.4 mm was used for the scanning purpose. Thickness of all films was measured by using cross sectional scanning electron microscope (SEM) images. The chemical bonding information of the thin films was analyzed by using FT-IR spectrometer (IR Affinity-1S, Shimadzu, Japan). The optical transmittance spectra of the nano crystal thin films were done using a UV-Vis spectrophotometer (V-770, Jasco, Japan).

2 Results and Discussion

2.1 EDAX Analysis

The elemental analysis of undoped and Cu doped ZnO thin films has been investigated by using EDAX. The x_{Cu} in the deposited ZnO thin films was confirmed by EDAX. EDAX spectra of undoped and 6.5% Cu doped ZnO thin films are shown in Fig. 1.

The sharp peak intensities of Zn and O were found in the undoped thin films, which confirmed the ZnO thin films by EDAX. Zn and O peaks with the additional Cu peak were observed in the Cu doped ZnO, as shown in Fig. 1(b). In the undoped thin films, Zn and O were the major intense peaks, but in Cu doped film, Cu was a minor intense peak, which incorporated with Zn host matrix and also substituted in Zn^{2+} ion sites in EDAX spectra.

2.2 XRD Study

The nature of crystallization characteristics of the undoped and Cu doped ZnO thin films has been investigated by XRD analysis. The XRD patterns of undoped and Cu doped ZnO thin films were recorded in 2θ between 20° to 70° using Cu-K_α radiation of wavelength $\lambda = 1.540\,6$ Å, where the source voltage and current were kept at 40 kV and 40 mA respectively as shown in Fig. 2. Herein, θ is also the Bragg's angle or glancing angle. The XRD spectra of the deposited films were done with a scan rate of 2°/min. All synthesized films were classified on the basis of their crystal structures, which depend on the condition of some deposition parameters. Naturally, the crystal structures of ZnO and Cu doped ZnO nano range films are two types, hexagonal wurtzite and cubic zinc blende[2-4,8,22]. The high

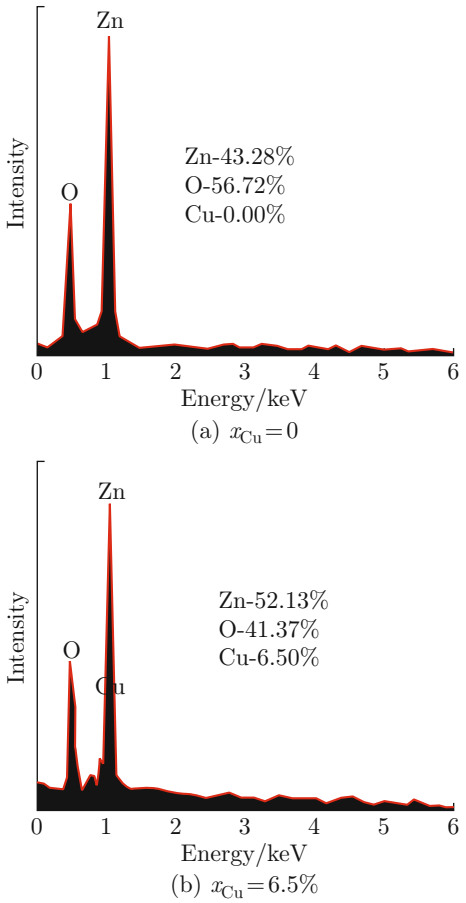

Fig. 1 EDAX spectra of Cu doped ZnO thin films

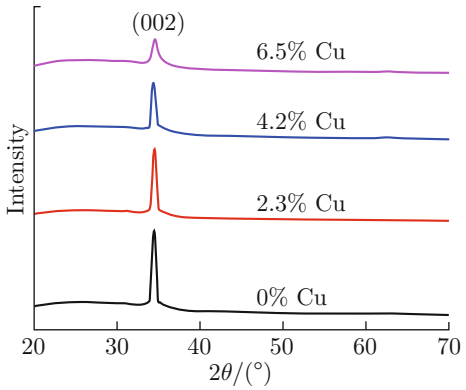

Fig. 2 XRD patterns of different x_{Cu} doped ZnO thin films deposited on glass substrates

intensity peak at 2θ of 34.44° corresponding to Miller indices (002) confirmed that the ZnO wurtzite hexagonal peak matched with JCPDS card No. 36-1451[10,13], which was decreased slowly with the increase of x_{Cu} from 0 to 6.5% respectively[2,22]. The crystallite sizes (D) of the deposited films were measured by using Debye-Scherrer equation[2,13]:

$$\frac{1}{D} = \frac{\beta \cos\theta}{K\lambda}, \tag{1}$$

where K is a Scherer constant and its value is 0.94, λ is the wavelength of X-ray and its value is 1.540 6 Å, and β is the full width at half maximum. The crystallite size of the deposited films on the glass substrate decreased from 27 nm to 22 nm with the increase of x_{Cu} from 0 to 6.5% respectively. The crystallite size of the deposited thin films decreased with predominant shifting of Cu^{2+} ions into the ZnO host lattice sites, which minimizes the nucleation and successive growth rate by increasing the x_{Cu} in the ZnO films. As the crystallite size was inversely proportional to the β, then the crystallite size decreased from 27 nm to 22 nm with the increase of β ranging from 0.317 2° to 0.389 1° respectively[13]. The strains (ε) of the deposited thin films were measured by[13]

$$\varepsilon = \frac{\beta}{4}\cos\theta. \tag{2}$$

The strain of the deposited thin films increased from 13.2×10^{-4} to 16.2×10^{-4} with the increase of x_{Cu} from 0 to 6.5% respectively. The strain of the deposited thin films increased due to the increase of copper ion inside the film[2].

The crystalline interplanar spacing (d) of the deposited thin films was calculated using Bragg's equation[3]:

$$d = n\lambda/(2\sin\theta), \tag{3}$$

where n is an order of diffraction. The lattice constant c of deposited films was calculated by[3]

$$d^{-2} = [4(h^2+hk+k^2)/(3a^2)] + l^2/c^2, \tag{4}$$

where a and c are lattice constants; h, k and l are Miller indices. The lattice constant c of the deposited films changes slightly from 5.202 Å to 5.216 Å due to the substitution of Cu^{2+} ion instead of Zn^{2+} ion at their respective lattice sites. It was clearly observed that an increase in strain causes decrease in crystallite size and increase in lattice constants[13]. The values of 2θ, β, D, ε, d and c for undoped and Cu doped ZnO thin films are shown in Table 2.

Table 2 X-ray diffraction data of Cu doped ZnO thin films at different x_{Cu}

x_{Cu}/%	2θ/(°)	β/(°)	D/nm	d/Å	$\varepsilon\times10^4$	c/Å
0	34.44	0.317 2	27	2.601	13.21	5.202
2.3	34.42	0.323 4	27	2.603	13.47	5.206
4.2	34.39	0.356 7	25	2.606	14.86	5.212
6.5	34.38	0.389 1	22	2.608	16.21	5.216

2.3 Atomic Force Microscopy Analysis

The surface morphology of undoped and Cu doped ZnO thin films has been investigated by scanning probe AFM. The high resolution AFM micrograph shows that the immaculate film has found to be homogeneous and uniform. Two-dimensional AFM images of undoped and Cu doped ZnO thin films are shown in Fig. 3. The surface morphology of the deposited nano crystal thin films varies with the variation of x_{Cu}. The good surface morphology of the deposited nano range thin films is a significant reason for the transmittance of light, which may be the scattering and reflecting from their rough surfaces. The decreases in surface roughness with the increase of x_{Cu} from 0 to 6.5% were combined with the decrease in grain size. It was evident that the different deposition of x_{Cu} modified the grain sizes and surface roughness. Grain sizes varied from 23 nm to 12 nm, which was comparable with the grain size as calculated from XRD data.

2.4 FT-IR Study

FT-IR spectra of undoped and Cu doped ZnO nano range thin films deposited on glass substrate were observed to analyze the chemical composition at room

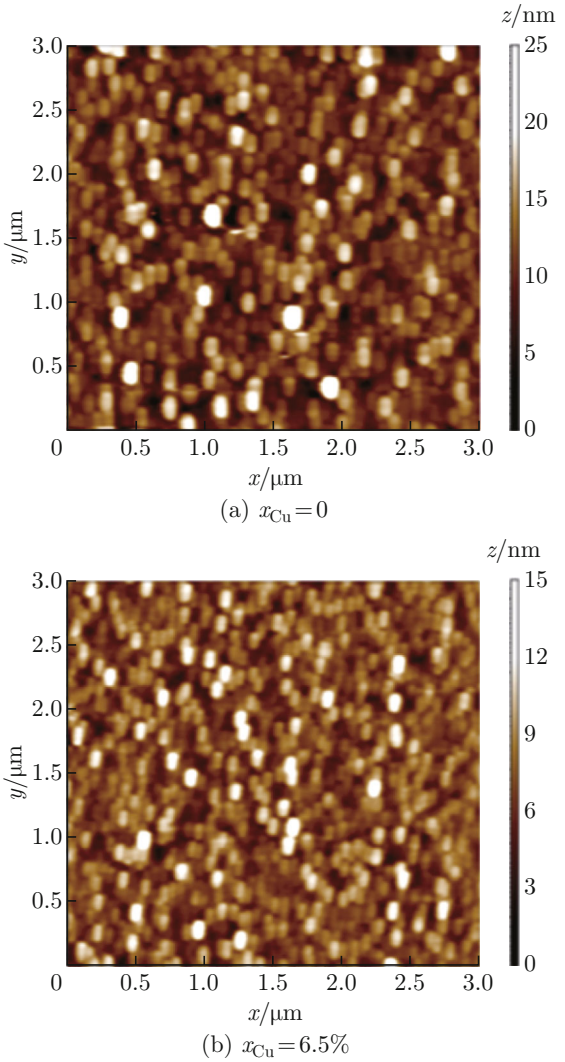

Fig. 3 Two-dimensional AFM images of Cu doped ZnO thin films

temperature of 30 °C in the frequency ranging from 400 cm^{-1} to 4 000 cm^{-1}, as shown in Fig. 4. Glass substrate was used as reference for measuring the FT-IR absorption spectra to eliminate the absorption peak due to glass substrate. The FT-IR spectra were used to analyze the structural and molecular arrangements in the undoped and Cu doped ZnO thin films. The FT-IR frequency in the range of wave number between 400 cm^{-1} to 4 000 cm^{-1} can be classified as the fingerprint region, which is 400 cm^{-1} to 1 600 cm^{-1} and the functional group region, which is 1 600 cm^{-1} to 4 000 cm^{-1} respectively. The stretching and bending vibration occurs between the fingerprint region and the functional group region. The FT-IR peaks are found due to the stretching and bending vibration of atom and molecules or functional groups. The intensity of the different bond peaks depends on different materials. The intensity of few peaks increased with the increase of x_{Cu} within ZnO from 0 to 6.5%. A sharp absorption peak found at near 455 cm^{-1} was assigned to stretching frequency for Zn—O bond in the thin films, which also confirmed the deposited ZnO thin films[23-24].

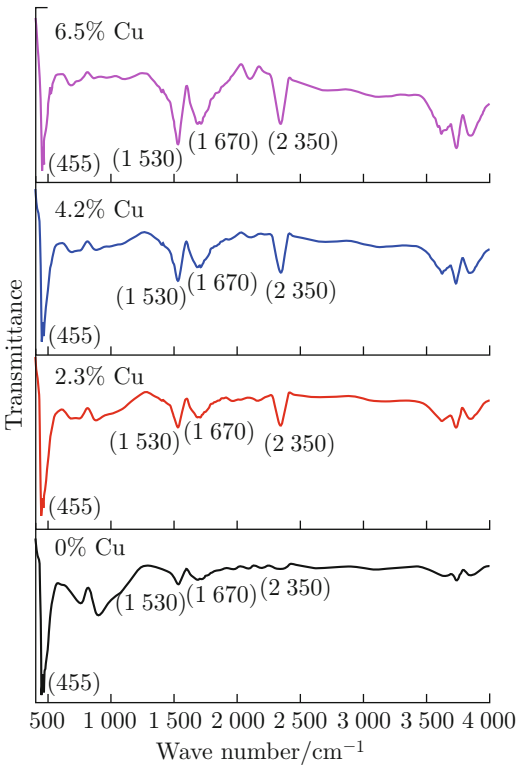

Fig. 4 FT-IR spectra of Cu doped ZnO thin films

The band found close to 530 cm^{-1} was assigned for the stretching vibration of CuO phonon spectrum, which increased with the increase of x_{Cu} from 2.3% to 6.5% in the ZnO films[25]. Due to the phonon spectrum of Cu_2O, one stretching absorption peak was found at around 616 cm^{-1}, which increased very slowly with the increase of x_{Cu} from 2.3% to 6.5%[25-26]. The strong absorption FT-IR peak was near 1 530 cm^{-1}, assigned for the symmetric strong C═O band[27-28]. A weak intensity peak was also found near 1 670 cm^{-1}, which can be attributed to asymmetric C═O bond[28]. The clear absorption peak was observed near 2 350 cm^{-1}, assigned for the CO_2 molecules in the thin films during the deposition of the thin films or atmospheric CO_2 molecules[29-30]. The broad double absorption peak was found in the range of wave number between 3 730 cm^{-1} to 3 860 cm^{-1}, which was due to O—H or C—H stretching vibrations of hydroxyl groups presented in thin films or due to the atmosphere during the FT-IR analysis[1,28].

2.5 Optical Study

Optical studies of undoped and Cu doped ZnO thin films deposited on the glass substrate were performed by using UV-Vis spectrophotometer at room temperature in the wavelength range of 200—800 nm, as shown in Fig. 5(a). The films showed a very high average of transmittance (90%) in the visible region, which indicates that the films are in good quality of optical properties due to low scattering or absorption losses. The transmittance spectra of thin films moderately decrease with the increase of x_{Cu} within pure ZnO, as shown in Fig. 5(a); they shift from visible region to near UV region. The decrease of optical transmittance may be due to the increase in film thickness[31]. The thickness of the deposited films increased from 230 nm to 310 nm, which is calculated from cross-sectional SEM images. From the band theory of solids, the absorption coefficient (α) can be calculated by Beer-Lambert law[3,32]:

$$I_t = I_0 e^{-\alpha t}, \tag{5}$$

where α is the absorption coefficient, I_0 and I_t are the incident and transmitted light intensities respectively, and t is the film thickness. The transmittance relation can be written as $T = I_t/I_0$ from simplifying formula of Beer-Lambert equation. The optical band gap energy of undoped and Cu doped ZnO thin films is determined by the fitting data absorption coefficient from the Tauc expression[32-34]:

$$(\alpha h\nu)^{1/m} = B(h\nu - E_g), \tag{6}$$

where B is a constant, $h\nu$ is the incident photon energy (h is Planck's constant and ν is incident light frequency), E_g is the optical band gap energy which varies with different deposition materials, and m is the different types of transition value. As ZnO is a semiconductor material with a direct allowed band gap, so for this case the value of m is 0.5[3]. In the case of direct allowed transition, the optical band gap energy (E_g) of Cu doped ZnO thin films was obtained from the extrapolation of the straight line on the x-axis using $(\alpha h\nu)^2$ versus $h\nu$ graph as shown in Fig. 5(b). It is seen that

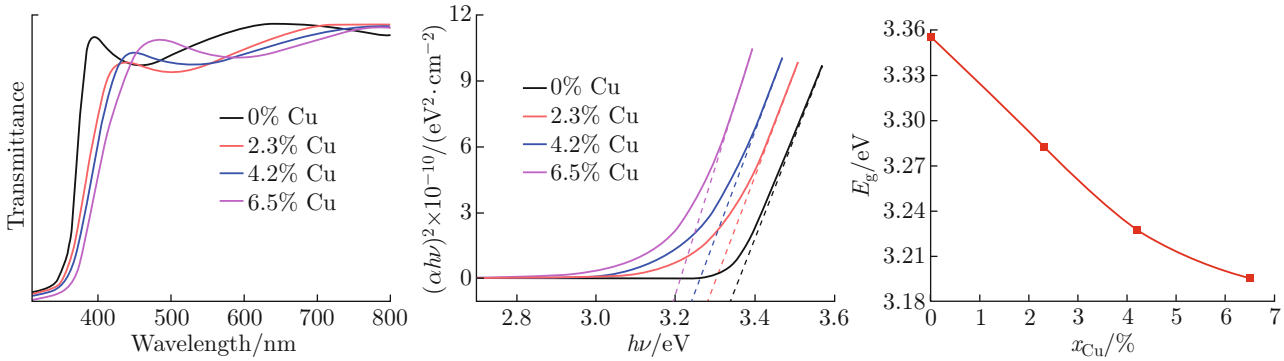

(a) Transmission spectra of Cu doped ZnO thin films with the variation of x_{Cu}

(b) Tauc plot of $(\alpha h\nu)^2$ vs. $h\nu$ at a different x_{Cu}

(c) Variation of E_g with x_{Cu}

Fig. 5 Results of optical study

the optical band gap energy of the nano crystal thin films reduced slowly with entering Cu into the ZnO layer. The energy levels of 2p of O and 3d of Cu were aligned simultaneously and also interchanged between the bands[35-36]. As a result, the hybridization that occurred between the bands Cu 3d and O 2p caused the decrease in the band gap of Cu doped ZnO nano range thin films, which is shown in Fig. 5(b). For different x_{Cu} doped ZnO samples, the excitonic absorption indicates that the energy band gap (E_g) values decrease with the increase of Cu^{2+} ion content. Figure 5(c) shows the decreasing values of band gap energy with respect to the increase of x_{Cu}.

2.6 Urbach Energy Analysis

Urbach energy is also known as "band tail width" associated with localized energy states due to structural disorder of crystals. Figure 6(a) shows the schematic diagram of Urbach band tail for Cu doped ZnO thin films. The Urbach energy relation is expressed by

$$E_u = \Delta E_g - \Delta E_{g'}, \tag{7}$$

where E_u is Urbach energy, ΔE_g is the energy gap between valance band and conduction band, and $\Delta E_{g'}$ is the energy gap between valance band tail and conduction band tail. The E_u, which is determined by fitting an exponential function to the slope of the absorption edge, gives the disorder or defect density[37-38]. The E_u also shows the phonon states of disorder in the deposited thin films. The E_u of band tail width is found to be below the absorption band edge of the compound. The generation of absorption edge at the band gap energy is due to exciting-phonon interaction or may be due to electron-phonon interaction.

This can be estimated from the steepness parameter of absorption edge which is usually credited to the optical-electronic transitions between the excited states and the near edge localized states. The band bending is due to a reduction in the optical band gap. If the E_u is higher, the disorder of the film is also high in phonon state. Urbach band tail is also expressed by[4,32,39]

$$\ln\alpha = \ln\alpha_0 - h\nu/E_u, \tag{8}$$

where α_0 is a constant.

The Urbach energy (E_u) shows that the width of the band tail is due to the presence of localized states in the band gap. The Urbach tail of Cu doped ZnO thin films was calculated from the slope of $\ln\alpha$ versus $h\nu$ plotted in Fig. 6(b).

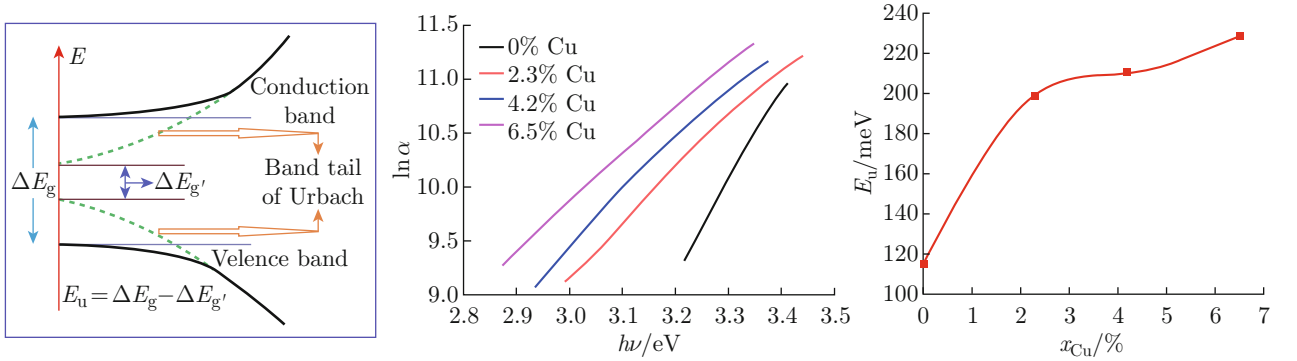

(a) Schematic diagram of Urbach band tail

(b) A plot of $\ln\alpha$ vs. $h\nu$ of Cu doped ZnO thin films

(c) Variation of Urbach energy (E_u) of Cu doped ZnO thin films with x_{Cu}

Fig. 6 Results of Urbach energy analysis

The Urbach energy directly provides some useful message about the thermal disorder or the occupancy level in the crystalline structure of phonon states[38]. The exponential increase of the absorption coefficient (α) in the range of the absorption edge can be explained from the transitions between the tails of the density of states in the conduction band and the valence band, and the shape and size of these tails. According to Skettrup's theory, the structural and thermal disorder in the sample could be calculated, which is modelled as an Einstein oscillator[38]. Generally, the optical band gap of thin films is inversely related with E_{u}. The E_{u} increases with the increase of x_{Cu} from 0 to 6.5% within ZnO. The Urbach energy increases from 115 meV to 228 meV with the increase of x_{Cu} from 0 to 6.5% within ZnO, which is shown in Fig. 6(c). The disorder of the deposited nano range thin films increases with the increase in Urbach energy. The increase of E_{u} suggests that the redistribution of states is from tail to tail and band to tail transitions, and severally, the optical band gap decreases owing to the enlargement of the Urbach tail[40].

3 Conclusion

In this research, Cu doped ZnO nano crystal thin films have been deposited on the glass substrates via reactive co-sputtering technique. Structural crystallinity of the deposited nanostructure thin films was characterized by using XRD. The chemical composition of the atoms and molecules in the deposited films was analyzed by using FT-IR spectrometer in the range of wave number from 400 cm^{-1} to 4 000 cm^{-1} at the transmittance band. The morphological property of the deposited films was characterized by using AFM. The optical band gap energy of Cu doped ZnO thin films decreases from 3.35 eV to 3.19 eV with the increase of x_{Cu} from 0 to 6.5% at room temperature of 30 °C. Urbach energy increases from 115 meV to 228 meV with the increase of x_{Cu} from 0 to 6.5% at room temperature of 30 °C. The potential advantage of Cu doped ZnO thin films as an optical coating can be taken with controlling its transparency and optical band gap by changing the Cu content independently from other parameters.

References

[1] SAJJAD M, ULLAH I, KHAN M I, et al. Structural and optical properties of pure and copper doped zinc oxide nanoparticles [J]. *Results in Physics*, 2018, **9**: 1301-1309.

[2] IMRAN M, AHMAD R, AFZAL N, et al. Copper ion implantation effects in ZnO film deposited on flexible polymer by DC magnetron sputtering [J]. *Vacuum*, 2019, **165**: 72-80.

[3] YUSOF A S, HASSAN Z, ZAINAL N. Fabrication and characterization of copper doped zinc oxide by using co-sputtering technique [J]. *Materials Research Bulletin*, 2018, **97**: 314-318.

[4] MAITI U N, GHOSH P K, AHMED S F, et al. Structural, optical and photoelectron spectroscopic studies of nano/micro ZnO: Cd rods synthesized via sol-gel route [J]. *Journal of Sol-Gel Science and Technology*, 2007, **41**(1): 87-92.

[5] MUKHERJEE N, AHMED S F, CHATTOPADHYAY K K, et al. Role of solute and solvent on the deposition of ZnO thin films [J]. *Electrochimica Acta*, 2009, **54**(16): 4015-4024.

[6] CAGLAR Y, CAGLAR M, ILICAN S, et al. Effect of channel thickness on the field effect mobility of ZnO-TFT fabricated by sol gel process [J]. *Journal of Alloys and Compounds*, 2015, **621**: 189-193.

[7] AL-HARDAN N H, ABDULLAH M J, AHMAD H, et al. Investigation on UV photodetector behavior of RF-sputtered ZnO by impedance spectroscopy [J]. *Solid-State Electronics*, 2011, **55**(1): 59-63.

[8] KHOSRAVI P, KARIMZADEH F, SALIMIJAZI H R, et al. Structural, optical and electrical properties of co-sputtered p-type ZnO: Cu thin-films [J]. *Ceramics International*, 2019, **45**(6): 7472-7479.

[9] KIM H, PIQUÉ A, HORWITZ J S, et al. Effect of aluminum doping on zinc oxide thin films grown by pulsed laser deposition for organic light-emitting devices [J]. *Thin Solid Films*, 2000, **377/378**: 798-802.

[10] ZARGAR R A, KHAN S U D, KHAN M S, et al. Synthesis and characterization of screen printed $Zn_{0.97}Cu_{0.03}O$ thick film for semiconductor device applications [J]. *Physics Research International*, 2014, **2014**: 464809.

[11] ISHERWOOD P J M. Copper zinc oxide: Investigation into a p-type mixed metal oxide system [J]. *Vacuum*, 2017, **139**: 173-177.

[12] PANDEY B, GHOSH S, SRIVASTAVA P, et al. Synthesis of nanodimensional ZnO and Ni-doped ZnO thin films by atom beam sputtering and study of their physical properties [J]. *Physica E*: *Low-Dimensional Systems and Nanostructures*, 2009, **41**(7): 1164-1168.

[13] MUTHUKUMARAN S, GOPALAKRISHNAN R. Structural, FTIR and photoluminescence studies of Cu doped ZnO nanopowders by co-precipitation method [J]. *Optical Materials*, 2012, **34**(11): 1946-1953.

[14] GHOMRANI F Z, AISSAT A, ARBOUZ H, et al. Al concentration effect on ZnO based thin films: For photovoltaic applications [J]. *Energy Procedia*, 2015, **74**: 491-498.

[15] SREEDHAR A, KWON J H, YI J, et al. Enhanced photoluminescence properties of Cu-doped ZnO thin films deposited by simultaneous RF and DC magnetron sputtering [J]. *Materials Science in Semiconductor Processing*, 2016, **49**: 8-14.

[16] YAO C B, WEN X, LI Q H, et al. The saturable absorption and reverse saturable absorption properties of Cu doped zinc oxide thin films [J]. *Chemical Physics Letters*, 2017, **671**: 113-117.

[17] AYDOGU S, SENDIL O, COBAN M. The optical and structural properties of ZnO thin films deposited by the spray pyrolysis technique [J]. *Chinese Journal of Physics*, 2012, **50**(1): 89-100.

[18] GHOSH A, GHULE A, SHARMA R. Effect of Cu doping on LPG sensing properties of soft chemically grown nano-structured ZnO thin film [J]. *Journal of Physics*: *Conference Series*, 2012, **365**: 012022.

[19] SHUKLA R K, SRIVASTAVA A, KUMAR N, et al. Optical and sensing properties of Cu doped ZnO nanocrystalline thin films [J]. *Journal of Nanotechnology*, 2015, **2015**: 172864.

[20] MAITI U N, AHMED S F, MITRA M K, et al. Novel low temperature synthesis of ZnO nanostructures and its efficient field emission property [J]. *Materials Research Bulletin*, 2009, **44**(1): 134-139.

[21] AZUMA M, ICHIMURA M. Fabrication of ZnO thin films by the photochemical deposition method [J]. *Materials Research Bulletin*, 2008, **43**(12): 3537-3542.

[22] CHICHVARINA O, HERNG T S, PHUAH K C, et al. Stable zinc-blende ZnO thin films: Formation and physical properties [J]. *Journal of Materials Science*, 2015, **50**(1): 28-33.

[23] KHAN M, AHMED S F. Effect of distance between cathode and substrate on structural and optical properties of zinc oxide thin films deposited by RF sputtering technique [J]. *Materials Physics and Mechanics*, 2021, **47**: 872-884.

[24] BABU K S, REDDY A R, SUJATHA C, et al. Synthesis and optical characterization of porous ZnO [J]. *Journal of Advanced Ceramics*, 2013, **2**(3): 260-265.

[25] JOHAN M R, SUAN M S M, HAWARI N L, et al. Annealing effects on the properties of copper oxide thin films prepared by chemical deposition [J]. *International Journal of Electrochemical Science*, 2011, **6**: 6094-6104.

[26] SERIN N, SERIN T, HORZUM S, et al. Annealing effects on the properties of copper oxide thin films prepared by chemical deposition [J]. *Semiconductor Science and Technology*, 2005, **20**(5): 398-401.

[27] FATTAH Z A. Synthesis and characterization of nickel doped zinc oxide nanoparticles by sol-gel method [J]. *International Journal of Engineering Sciences and Research Technology*, 2016, **5**: 418-429.

[28] KHAN Z R, KHAN M S, ZULFEQUAR M, et al. Optical and structural properties of ZnO thin films fabricated by sol-gel method [J]. *Materials Sciences and Applications*, 2011, **2**(5): 340-345.

[29] HAO Y M, LOU S Y, ZHOU S M, et al. Structural, optical, and magnetic studies of manganese-doped zinc oxide hierarchical microspheres by self-assembly of nanoparticles [J]. *Nanoscale Research Letters*, 2012, **7**(1): 100.

[30] KAYANI Z N, IQBAL M, RIAZ S, et al. Fabrication and properties of zinc oxide thin film prepared by Sol-gel dip coating method [J]. *Materials Science-Poland*, 2015, **33**(3): 515-520.

[31] SHUKLA R K, KUMAR N, SRIVASTAVA A, et al. Optical and sensing properties of Al doped ZnO nanocrystalline thin films prepared by spray pyrolysis [J]. *Materials Today*: *Proceedings*, 2018, **5**(3): 9102-9107.

[32] KHAN M, ALAM M S, SAHA B, et al. Synthesis and characterization of cadmium sulfide (CdS) thin films by cyclic voltammetry technique [J]. *Materials Today*: *Proceedings*, 2021, **47**: 2351-2357.

[33] CHUNG S M, SHIN J H, LEE J M, et al. Structural and optical properties of Cu doped ZnO thin films by co-sputtering [J]. *Journal of Nanoscience and Nanotechnology*, 2011, **11**(1): 782-786.

[34] AHMED S F, KHAN S, GHOSH P K, et al. Effect of Al doping on the conductivity type inversion and electro-optical properties of SnO_2 thin films synthesized by sol-gel technique [J]. *Journal of Sol-Gel Science and Technology*, 2006, **39**(3): 241-247.

[35] FERHAT M, ZAOUI A, AHUJA R. Magnetism and band gap narrowing in Cu-doped ZnO [J]. *Applied Physics Letters*, 2009, **94**(14): 142502.

[36] MURSAL, IRHAMNI, BUKHARI, et al. Structural and optical properties of zinc oxide (ZnO) based thin films deposited by Sol-gel spin coating method [J]. *Journal of Physics*: *Conference Series*, 2018, **1116**: 032020.

[37] RAI R C. Analysis of the Urbach tails in absorption spectra of undoped ZnO thin films [J]. *Journal of Applied Physics*, 2013, **113**(15): 153508.

[38] ISLAM M A, HOSSAIN M S, ALIYU M M, et al. Comparison of structural and optical properties of CdS thin films grown by CSVT, CBD and sputtering techniques [J]. *Energy Procedia*, 2013, **33**: 203-213.

[39] AHMED S F, BANERJEE D, CHATTOPADHYAY K K. The influence of fluorine doping on the optical properties of diamond-like carbon thin films [J]. *Vacuum*, 2010, **84**(6): 837-842.

[40] VETTUMPERUMAL R, KALYANARAMAN S, SANTOSHKUMAR B, et al. Estimation of electron-phonon coupling and Urbach energy in group-I elements doped ZnO nanoparticles and thin films by sol-gel method [J]. *Materials Research Bulletin*, 2016, **77**: 101-110.